Three-dimensional polarization-independent visible-frequency carpet invisibility cloak

Joachim Fischer,[1,†] Tolga Ergin,[1,*,†] and Martin Wegener[1,2]

[1]*Institut für Angewandte Physik and DFG-Center for Functional Nanostructures (CFN), Karlsruhe Institute of Technology (KIT), Wolfgang-Gaede-Straße 1, D-76131 Karlsruhe, Germany*

[2]*Institut für Nanotechnologie, Karlsruhe Institute of Technology (KIT), D-76021 Karlsruhe, Germany*

**Corresponding author: tolga.ergin@kit.edu*

Received March 8, 2011; revised April 27, 2011; accepted April 28, 2011; posted April 29, 2011 (Doc. ID 143769); published May 27, 2011

We miniaturize all features in a previously introduced polarization-independent three-dimensional carpet invisibility cloak by more than a factor of 2. This leads to operation wavelengths in the visible. The structures are characterized by electron and optical microscopy. In contrast to our previous work at IR wavelengths, we can directly measure two-dimensional images at visible frequencies, perform control experiments from the backside, and compare the images with theory. We find excellent agreement. Furthermore, we study the wavelength dependence in the range from 900 nm down to 500 nm. Cloaking action deteriorates as the woodpile stop band at around 575 nm is approached. © 2011 Optical Society of America

OCIS codes: 230.3205, 160.3918, 080.2710, 160.1245, 160.5298.

Transformation optics can be viewed as a powerful tool for designing optical systems. The strength of this tool is emphasized by invisibility cloaking [1–3], which was long believed to be impossible. In particular, the carpet-cloak concept [4] has inspired experiments by several groups [5–13]. In brief, by tailoring a refractive-index profile, the carpet cloak makes a bump in a metal mirror (the carpet) appear flat. This allows for hiding objects underneath this carpet. However, the "Holy Grail" of a macroscopic three-dimensional (3D) cloak for unpolarized visible light has not been accomplished so far. Our 2010 work [9] demonstrated a microscopic 3D carpet cloak for unpolarized light down to wavelengths of about 1.5 μm. More recent work [12,13] by other groups has demonstrated macroscopic carpet cloaks at visible frequencies, however, only for one linear polarization of light (due to the birefringent calcite used) and in an effectively two-dimensional configuration.

In this Letter, we miniaturize our 2010 structure by more than a factor of 2, leading to what we believe to be the first 3D carpet cloak for unpolarized visible light. This also allows for refined characterization via optical microscopy. Comparison with ray-tracing calculations shows that the cloaking performance is close to the theoretical expectation.

The polymer structures in this work are fabricated by stimulated-emission-depletion (STED)-inspired direct laser writing, closely following along the lines of our Ref. [14], with two modifications. First, we employ a different photoinitiator in a similar monomer, i.e., 0.25 wt. % 7-diethylamino-3-thenoylcoumarin in pentaerythritol tetraacrylate. This ketocoumarin offers a better ratio between depletion efficiency and undesired absorption of the 532 nm cw depletion laser (which limits resolution). Second, we not only improve the lateral but also the axial resolution by using a suitable phase mask known from STED microscopy [15]. After exposure, the photoresist structures are developed in 2-propanol and dried supercritically with CO_2(Leica EM CPD030).

As in previous work [9], the refractive-index profile of the carpet cloak calculated from the quasi-conformal mapping [4] is mimicked by adjusting the local volume filling fraction of a 3D polymer woodpile photonic crystal. Here, this is achieved by varying the excitation power while keeping the depletion power fixed. In our 2010 experimental work [9], we succeeded in fabricating a 3D carpet-cloak device with a rod spacing of $a = 800$ nm. Here, to allow for direct comparison, we fabricate a miniaturized version with $a = 350$ nm. Because of the scalability of the Maxwell equations, the operation wavelength is expected to scale from the lower limit of about 1.5 μm in Ref. [9] down to $1.5\,\mu\text{m} \times 350\,\text{nm}/800\,\text{nm} = 0.7\,\mu\text{m}$, i.e., to visible red light.

Corresponding results are depicted in Fig. 1. Figure 1(a) shows an oblique-view electron micrograph of a homogeneous woodpile photonic crystal (the "reference") as well as of the carpet cloak structure itself. After completing optical lithography, the samples are coated with a 100 nm thick gold film in a sputter chamber (Cressington 108 auto). To enhance the visibility of details in Fig. 1(a), we have overlaid two scanning electron micrographs with different brightness (high dynamic range image). The gold parts are colored in yellow, the polymer parts in blue. The overall design dimensions of each structure are $50\,\mu\text{m} \times 20\,\mu\text{m} \times 5\,\mu\text{m}$, the latter corresponding to 40 layers of polymer rods. The full width of the $\cos^2$-shaped bump is 6 μm, and its height is 0.5 μm. The oblique-view (54° tilt with respect to surface normal) electron micrographs taken after focused-ion-beam milling and shown in Fig. 1(b) reveal the 3D interior of two structures nominally identical to the measured ones.

To investigate the resulting effective optical properties, we have taken true-color reflection optical micrographs from the air side, Fig. 1(c), and from the glass-substrate side, Fig. 1(d), using an optical microscope (ZEISS objective LD Achroplan, 20, NA = 0.4). We have previously shown by numerical modeling [11] that characterization with larger numerical apertures approaching unity leads to a less sensitive test of the cloaking performance. A laser (Spectra Physics Inspire) operating at 700 nm wavelength, sent through a rotating diffuser, serves for the illumination. Both linear polarizations lead to similar results

(not depicted); here we show data for circular polarization. Under the present conditions, circular illumination is effectively equivalent to unpolarized illumination. Note the two pronounced dark stripes due to the bump for the reference and the cloak in Fig. 1(c) when inspected from the air side, which serves as a control experiment. When inspected from the glass-substrate side, the reference structure (top) still shows these pronounced dark stripes. In sharp contrast, the stripes almost completely disappear for the cloaking structure (bottom).

To investigate different viewing angles, we rotate the samples along the bump axis by 30° ("dark-field mode") and repeat the optical experiments. The result shown in Fig. 2 exhibits pronounced scattering of light off of the

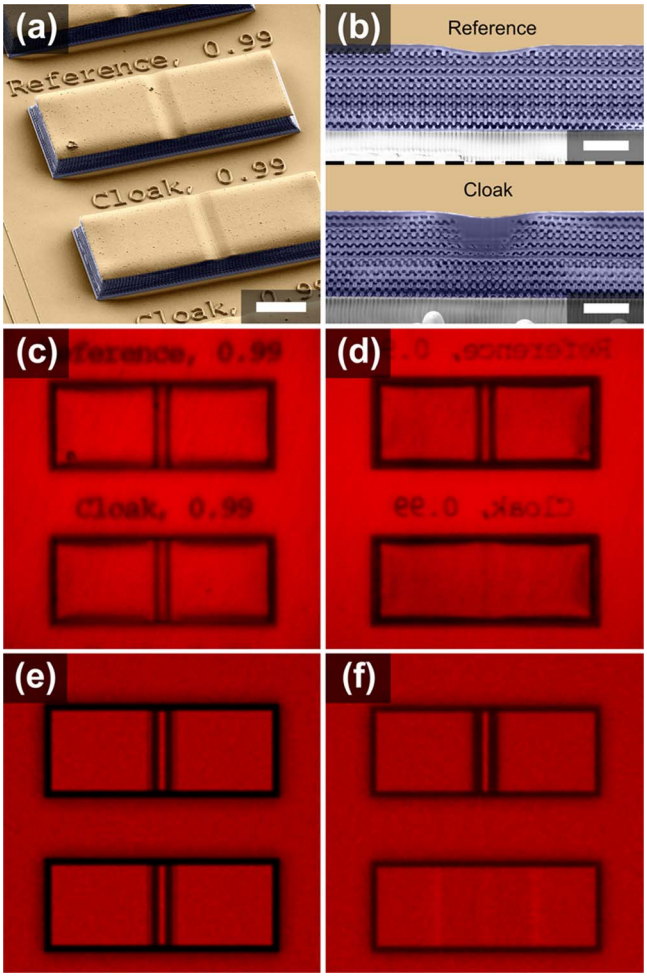

Fig. 1. (Color online) (a) Colored oblique-view electron micrograph of the polymer reference (top) and carpet cloak (bottom) structures (fabricated on glass substrate and coated with 100 nm gold). The scale bar corresponds to 10 μm. (b) Corresponding focused-ion-beam cuts of nominally identical structures. The scale bar corresponds to 2 μm. (c) and (d) are true-color optical micrographs of the structures in (a) taken with an optical microscope under circularly polarized illumination at 700 nm wavelength. Note the identical distortions due to the bump in both structures in (c) when inspected from the air side (serving as a control experiment). When inspected from the glass-substrate side in (d), the reference structure (top) still shows pronounced dark stripes. In sharp contrast, the stripes essentially disappear for the cloaking structure (bottom). (e) and (f) are ray-tracing calculations corresponding to (c) and (d), respectively.

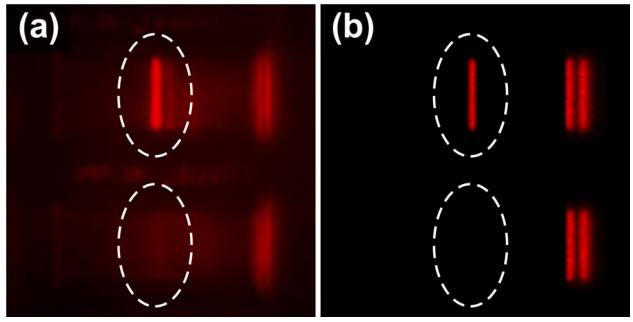

Fig. 2. (Color online) (a) As Fig. 1(d), but for rotation of the samples by 30° around an axis parallel to the bump. (b) Corresponding ray-tracing calculation. The white dashed ellipses highlight the bump region.

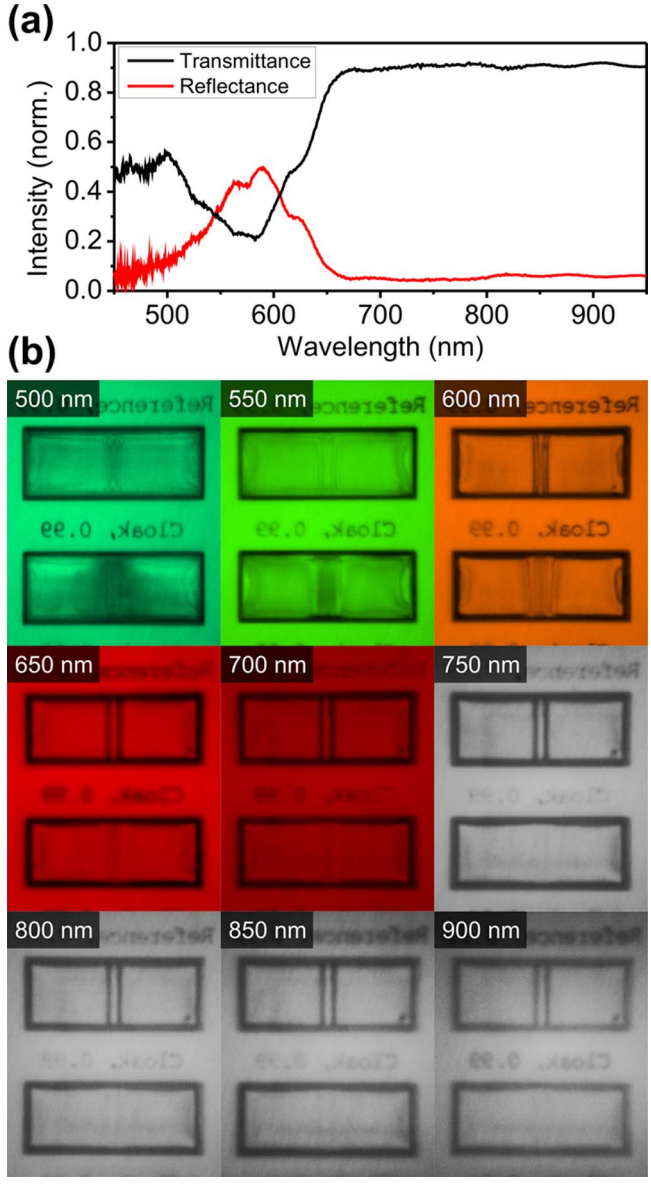

Fig. 3. (Color online) (a) Measured normal-incidence transmittance and reflectance spectra of the polymer woodpile taken on the reference structure before gold sputtering. (b) As Fig. 1 (d), but for different illumination wavelengths as indicated.

bump, whereas scattering is strongly suppressed for the cloaking structure.

All microscope images are in good agreement with detailed ray-tracing calculations. The details of the numerical approach can be found in Ref. [11]. Importantly, it accounts not only for the refractive-index profile of the ideal cloak, but also for the glass substrate, as well as the imaging process of the entire microscope. The good agreement between calculations and experiment indicates excellent sample quality.

It is interesting to investigate the wavelength dependence of the carpet cloak. Clearly, we expect that cloaking persists for wavelengths larger than 700 nm as long as the polymer remains transparent, which is the case up to about 3 μm. Deviations from the behavior of a simple effective medium and hence the end of cloaking action are expected if the wavelength approaches the stop band wavelength of the woodpile photonic crystal or if diffraction of light into the glass substrate sets in. These two conditions almost coincide under the present conditions. The normal-incidence intensity spectra measured on the reference structure on one side of the bump (taken before the gold sputtering) are shown in Fig. 3(a). A well pronounced stop band centered at around 575 nm is observed both in transmittance and in reflectance.

To investigate the wavelength dependence of the cloaking action, we repeat the bright-field-mode experiment shown in Fig. 1(d) at various other wavelengths. Corresponding data are depicted in Fig. 3(b). Cloaking is excellent for wavelengths in the range of 900 nm down to about 650 nm. For yet smaller wavelengths (e.g., 600 nm), distortions become gradually visible, i.e., cloaking no longer works. Notably, the bump itself is hardly visible for the reference structure at 550 nm. Here, the woodpile stop band reflects a major fraction of the light and, hence, the light never reaches the bump in the metal mirror. For the cloak at 550 nm, the inhomogeneous woodpile above the bump now leads to a dark zone.

In conclusion, we have fabricated and characterized what we believe to be the first 3D polarization-independent carpet cloak for visible light. The concepts of transformation optics combined with the fabrication technology used here might also allow for realizing other optical devices, e.g., unusual flat lenses [16].

We thank Nicolas Stenger and Georg von Freymann for many fruitful discussions. We acknowledge financial support provided by the Deutsche Forschungsgemeinschaft (DFG) and the State of Baden-Württemberg through the DFG-Center for Functional Nanostructures (CFN) within subprojects A1.4 and A1.5. The project PHOME acknowledges the financial support of the Future and Emerging Technologies (FET) programme within the Seventh Framework Programme for Research of the European Commission, under FET-Open grant number 213390. The project METAMAT is supported by the Bundesministerium für Bildung und Forschung (BMBF). The Ph.D. education of J. Fischer and T. Ergin is embedded in the Karlsruhe School of Optics & Photonics (KSOP).

[†]These authors have contributed equally to this work.

References

1. V. M. Shalaev, Science **322**, 384 (2008).
2. H. Chen, C. T. Chan, and P. Sheng, Nat. Mater. **9**, 387 (2010).
3. U. Leonhardt and T. G. Philbin, *Geometry and Light: The Science of Invisibility* (Dover, 2010).
4. J. Li and J. B. Pendry, Phys. Rev. Lett. **101**, 203901 (2008).
5. R. Liu, C. Ji, J. J. Mock, J. Y. Chin, T. J. Cui, and D. R. Smith, Science **323** 366 (2009).
6. J. Valentine, J. Li, T. Zentgraf, G. Bartal, and X. Zhang, Nat. Mater. **8**, 568 (2009).
7. L. H. Gabrielli, J. Cardenas, C. B. Poitras, and M. Lipson, Nat. Photon. **3**, 461 (2009).
8. J. H. Lee, J. Blair, V. A. Tamma, W. Wu, S. J. Rhee, C. J. Summers, and W. Park, Opt. Express **17**, 12922 (2009).
9. T. Ergin, N. Stenger, P. Brenner, J. B. Pendry, and M. Wegener, Science **328**, 337 (2010).
10. H. F. Ma and T. J. Cui, Nat. Commun. **1**, 21 (2010).
11. T. Ergin, J. C. Halimeh, N. Stenger, and M. Wegener, Opt. Express **18**, 20535 (2010).
12. B. Zhang, Y. Luo, X. Liu, and G. Barbastathis, Phys. Rev. Lett. **106**, 033901 (2011).
13. X. Chen, Y. Luo, J. Zhang, K. Jiang, J. B. Pendry, and S. Zhang, Nat. Commun. **2**, 176 (2011).
14. J. Fischer, G. von Freymann, and M. Wegener, Adv. Mater. **22**, 3578 (2010).
15. T. A. Klar, S. Jakobs, M. Dyba, A. Egner, and S. W. Hell, Proc. Natl. Acad. Sci. USA **97**, 8206 (2000).
16. D. R. Smith, Y. Urzhumov, N. B. Kundtz, and N. I. Landy, Opt. Express **18**, 21238 (2010).